Hindawi
Mathematical Problems in Engineering
Volume 2018, Article ID 4908459, 12 pages
https://doi.org/10.1155/2018/4908459

Research Article

H_∞ Control of Coronary Artery Input Time-Delay System via the Free-Matrix-Based Integral Inequality

Sha-sha Li,[1] Zhan-shan Zhao,[1] Jing Zhang,[2,3] Jie Sun,[1] and Lian-kun Sun[1]

[1]*School of Computer Science & Software Engineering, Tianjin Polytechnic University, Tianjin 300387, China*
[2]*School of Textiles, Tianjin Polytechnic University, Tianjin 300387, China*
[3]*Tianjin Vocational Institute, Tianjin 300410, China*

Correspondence should be addressed to Zhan-shan Zhao; zhzhsh127@163.com

Received 11 June 2017; Revised 16 October 2017; Accepted 6 November 2017; Published 16 January 2018

Academic Editor: R. Aguilar-López

The issue of H_∞ control for the coronary artery input time-delay system with external disturbance is of concern. To further reduce conservation, we utilize the free-matrix-based integral inequality, Wirtinger-based integral inequality, and reciprocal convex combination approach to construct Lyapunov-Krasovskii function (LKF). Then a sufficient condition for controller design which can guarantee robust synchronization the coronary artery system is represented in terms of linear matrix inequality (LMI). Finally, a numerical example is exploited to show the effectiveness of the proposed methods.

1. Introduction

As we all know, nonlinear dynamical systems have gotten increasing attraction in various fields researches [1–4]. As one of complex nonlinear dynamical systems, chaotic systems have been widely investigated because of their potential application in the model of chemical reaction, nervous systems, biological engineering systems, and so on [5–7]. Based on the feature of extreme sensitivity to initial conditions and the systems parameters for the chaotic systems, chaos synchronization has become a much more important task. The purpose of chaotic synchronization is to achieve synchronization of the slave and master systems, which leads the investigations of synchronization control to be a central topic. Up to now, many developed synchronization control schemes have been presented, such as feedback control [8], H_∞ control [9], sliding mode control [10], and impulsive control [11].

Nonlinear systems combined with biological engineering have become a hot issue. The intensive study of the coronary artery system as a practical biomathematical case of chaotic systems has significant meaning not only in clinic but also in engineering areas. From the clinic point of view, the purpose is to drive pathological vessel into the trajectory of healthy vessel to treat many complex cardiovascular diseases. From the engineering point of view, we demand a suitable synchronization controller to reduce undesired chaotic motion and achieve the synchronization of the two systems. In [12], to further lower the effect of external uncertainties, a chaos suppression controller was designed by sliding mode control to drive chaotic coronary artery system into the normal orbit, which can effectively reduce the probability of angina disease. A new terminal sliding mode control algorithm for synchronization of coronary artery system was proposed [13], which can ensure that trajectories of the spastic vessel asymptotically approach the ones of the normal vessel in finite time.

Input time-delay is likely to exist in modeling practical coronary artery system due to the speed of different patients absorbing the drug. The presence of input time-delay could degrade system performance and it may lead to vibration or chaotic behavior [14]. Therefore, it is very reasonable and necessary not only in practical applications but also in theory to investigate chaotic systems with input time-delay. In [15], the input time-delay was dealt by free matrix zero equality approach to achieve synchronization for chaotic Lur'e systems. The chaotic finance systems with input time-delay were proposed based on Jensen inequality [16]. The above-mentioned literature is still great exploring room in practical application. It is well known that the stability and synchronization of the considered systems with time

delay are often studied by introducing the LKF method, which can provide more useful state information and delay information. In order to reduce the possible conservatism of LKF method, many methods are proposed, such as the Jensen inequality [17], Wirtinger inequality [18], and free-matric-based integral inequality [19]. As a kind of earliest inequality, Jensen inequality was widely applied [20]. Because of avoiding the introduction of plentiful matrices, Jensen inequality was proposed to decrease much computational burden in [21]. In order to reduce Jensen's gap, Wirtinger inequality was regarded as an effective technique to improve the performance of time-delay systems [22, 23]. Then, free-matric-based integral inequality [24] had a wide application in stability analysis of time-delay systems due to its less conservatism than the above proposed inequality [21–23]. In addition, reciprocally convex combination can derive a stability condition with much less decision variables, which could achieve performance behavior identical to above approaches [25].

Motivated by above discussion, the issue of H_∞ control is further investigated for coronary artery input time-delay system with disturbance. The main contributions of this paper are presented as follows:

(1) An augmented LKF including double integral and triple integral terms is constructed, which can provide more valuable time-delay information. To get lower bound of $\int_{t-h}^{t}\int_{u}^{t} X(s)S_1X(s)ds\,du$ ($S_1 > 0$), the Wirtinger-based integral inequality is employed.

(2) Free-matric-based integral inequality and reciprocally convex combination are applied to reduce the enlargement in bounding the derivative of LKF as much as possible. Then, a state feedback controller subjecting to input time-delay is designed to guarantee asymptotical convergence to zero for the error system and reduce the effect of external disturbance to a prescribed H_∞ performance level. It means that the abnormal chaotic behavior of a coronary artery system is suppressed to a normal periodic orbit, which effectively relieves or eliminates angina symptoms.

The feasibility of the above strategy is illustrated based on a numerical example.

Main Structure. Section 2 describes the problem formulation and preliminaries; Section 3 provides the main proof result which could ensure orbit of chaotic coronary artery system with external disturbance asymptotically approaching the ones of normal system. Section 4 shows that the simulation result of the error system is asymptotical to approach zero. Section 5 reaches conclusion of chaotic synchronization.

Notation. R^n denotes n-dimensional Euclid space. $\|\cdot\|$ is the vector Euclid norm. $*$ is a diagonal of a symmetric matric. sym$\{Y\}$ indicates $Y + Y^T$.

2. Problem Formulation and Preliminaries

The chaotic behavior of blood vessel more easily resists external disturb than the sine periodic motion; thus the chaotic state of physiology system is a protection mechanism and is beneficial for normal blood vessel [26]. It is not always harmful and even is desired goal in some practical applications. In this paper, the main goal is to make the biomedical model of pathological blood vessel synchronize with a prescribed chaotic system of the normal vessel [27]. From the biological point of view, the purpose is to achieve synchronization between the chaotic states of pathological blood vessel and normal one. Some chaotic conditions may cause coronary artery obstruction and have an effect on transport of nutrients and oxygen to the heart which could result in coronary atherosclerosis and angina. In order to decrease those diseases morbidity, the synchronization of coronary artery system is investigated. Describe the mathematical model of the coronary artery system as follows in [12]:

$$\begin{aligned}\dot{x}_1(t) &= -cx_1 - dx_2,\\ \dot{x}_2(t) &= -(\tau + c\tau)x_1 - (\tau + d\tau)x_2 + \tau x_1^3 + E\cos\omega t,\end{aligned} \tag{1}$$

where x_1 and x_2 are state vector, which represent deviation of inner radius and pressure of vein, t is time variable, c, d, and τ are the coronary artery system parameters which satisfy $c\tau - \tau d > 0$, and more information can be obtained from [28]. The variation of the blood vessel radius and change of blood pressure could be affected with different c and d; chaos can be characterized by the static rheological characteristics of blood vessels caused with the change of τ [12]. $E\cos\omega t$ is disturbance term, which represents a period disturbance acting on the blood vessel from biological significance [29]. To simplify form of system (1), the healthy coronary artery system is presented as follows:

$$\dot{x}_m(t) = Ax_m(t) + Cf\left(x_m(t)\right) + v(t), \tag{2}$$

where matrices A and C depend on the value of c, d, and τ, $x_m(t) = [x_1, x_2]$, $f(x_m(t)) = [0, x_1^3]$, $v(t) = [0, E\cos\omega t]$.

The blood vessel in chaotic states may induce various complex diseases, for instance, myocardial infarction. With the purpose of suppressing the chaotic phenomenon of coronary artery system, we could design the feedback controller $u(t)$ to achieve the chaotic synchronization. The controller $u(t)$ is the dosage of the single and double nitrate isosorbide nitrate used for treatment of angina and other diseases [12]. We control the dosage of the single and double nitrate isosorbide nitrate to change blood vessel inner radius and pressure and achieve chaotic synchronization of normal and abnormal blood vessel, which can improve transport of nutrients and oxygen to the heart. The diseased system can be defined as the follows:

$$\begin{aligned}\dot{x}_s(t) = Ax_s(t) + Cf\left(x_s(t)\right) + v(t) + D\varrho(t)\\ + u(t - r(t)),\end{aligned} \tag{3}$$

where $x_s(t) = [x_{s1}(t), x_{s2}(t)]$ is the state vector, $f(x_s(t)) = [0, x_{s1}^3(t)]$ is nonlinear function vector, $v(t) = [0, E\cos\omega t]$ represents period disturbance, $\varrho(t) = [\varrho_1(t), \varrho_2(t)]$ represents uncertain external disturbance. Our intent is to synchronize the healthy and pathological coronary artery system, which means resulting tracking error need be driven to zero. Hence, defining $e(t) = x_s(t) - x_m(t)$, the error system based on (2) and (3) can be presented as follows:

$$\dot{e}(t) = Ae(t) + u(t - r(t)) + Cf(t) + D\varrho(t), \tag{4}$$

where input time-delay $r(t) \in [r_m, r_M]$, its derivative $\dot{r}(t) \leq r_d$, r_m, r_M, and r_d are given positive integers, $f(t) = f(x_s(t)) - f(x_m(t))$. Due to the time of drug absorption, we design the state feedback controller $u(t - r(t)) = K[x_s(t - r(t)) - x_m(t - r(t))]$ to achieve the synchronization of the normal and pathological coronary artery system. The error system can be obtained:

$$\dot{e}(t) = Ae(t) + Ke(t - r(t)) + Cf(t) + D\varrho(t). \quad (5)$$

In the paper, a controller obtained by feasible sets of K is designed to deal with the synchronization problem of chaotic coronary artery system. In other words, our goal is to drive pathological vessel into the trajectory of healthy vessel and ensure asymptotically approaching zero for the error system. To achieve the above proposed aim, we give the following assumption and lemmas.

Assumption 1. A constant matrix L with appropriate dimension satisfies

$$\left\| f(x_s(t)) - f(x_m(t)) \right\| \leq \left\| L(x_s(t) - x_m(t)) \right\|. \quad (6)$$

From (4), the following inequality can be obtained:

$$f^T(t) f(t) \leq L^T L e^T(t) e(t). \quad (7)$$

Lemma 2 (see [24]). *h is a continuously differentiable function: $[\vartheta_1, \vartheta_2] \to \mathbb{R}^n$. For symmetric matrices $R \in \mathbb{R}^{n*n}$, $M_1, M_3 \in \mathbb{R}^{3n*3n}$, and any matrices $M_2 \in \mathbb{R}^{3n*3n}$, $N_1, N_2 \in \mathbb{R}^{3n*n}$ are satisfying*

$$\begin{bmatrix} M_1 & M_2 & N_1 \\ * & M_3 & N_2 \\ * & * & Q \end{bmatrix} \geq 0. \quad (8)$$

We can obtain the following inequality:

$$\begin{aligned} &-\int_{\vartheta_1}^{\vartheta_2} \dot{h}^T(u) R \dot{h}(u)\, du \\ &\leq \omega_1^T (\vartheta_2 - \vartheta_1) \left[M_1 + \frac{1}{3} M_3 \right] \omega_1 \\ &\quad + \operatorname{sym}\left\{ \omega_1^T N_1 \omega_2 + \omega_1^T N_2 \omega_3 \right\}, \end{aligned} \quad (9)$$

where

$$\begin{aligned} \omega_1 &= \left[h^T(\vartheta_2), h^T(\vartheta_1), \frac{1}{\vartheta_2 - \vartheta_1} \int_{\vartheta_1}^{\vartheta_2} h^T(u)\, du \right]^T, \\ \omega_2 &= h^T(\vartheta_2) - h^T(\vartheta_1), \\ \omega_3 &= \frac{2}{\vartheta_2 - \vartheta_1} \int_{\vartheta_1}^{\vartheta_2} h^T(u)\, du - h^T(\vartheta_2) - h^T(\vartheta_1). \end{aligned} \quad (10)$$

Lemma 3 (see [30]). *Order matrix $V = V^T \geq 0$ and continuously differentiable function h in $[e, f] \to \mathbb{R}^n$. The following inequality holds:*

$$\int_e^f \dot{h}^T(u) V \dot{h}(u)\, du \geq \frac{1}{f - e} \left[\gamma_1 V \gamma_1 + \gamma_2 V \gamma_2 \right], \quad (11)$$

where

$$\begin{aligned} \gamma_1 &= h(f) - h(e), \\ \gamma_2 &= \sqrt{3}(e) + \sqrt{3}(f) - \frac{2\sqrt{3}}{f - e} \int_e^f h(u)\, du. \end{aligned} \quad (12)$$

Lemma 4 (see [25]). *In an open subset D of R^m, order positive value $L_i : \mathbb{R}^m \to R$. The reciprocally convex combination of L_i is satisfying*

$$\begin{aligned} &\min_{[b_i | b_i > 0, \sum_i b_i = 1]} \sum_i \frac{1}{b_i} L_i(t) = \sum_i L_i(t) + \max_{[K_{i,j}(t)]} \sum_{i \neq j} \\ &\text{subject to} \quad \left\{ K_{i,j} : \mathbb{R}^m \longrightarrow R, K_{i,j} \triangleq K_{i,j}(t), \begin{bmatrix} L_i(t) & K_{i,j}(t) \\ K_{i,j}(t) & L_j(t) \end{bmatrix} \geq 0 \right\}. \end{aligned} \quad (13)$$

Lemma 5 (see [22]). *Order matrix $W = W^T \geq 0$. For continuously differentiable function $h \in [b_1, b_2] \to \mathbb{R}^n$, we can obtain*

$$\begin{aligned} &\int_{b_1}^{b_2} \int_s^{b_2} \dot{h}^T(u) W \dot{h}(u)\, du\, ds \\ &\geq \frac{2}{(b_2 - b_1)^2} \left\{ \nu_1^T(b_1, b_2) W \nu_1(b_1, b_2) \right. \\ &\left. + \nu_2^T(b_1, b_2) W \nu_2(b_1, b_2) \right\}, \end{aligned} \quad (14)$$

where

$$\nu_1(b_1, b_2) = (b_2 - b_1) h(b_2) - \int_{b_1}^{b_2} h(s)\, ds, \quad (15)$$

$$\begin{aligned} \nu_2(b_1, b_2) &= \frac{\sqrt{2}(d_2 - d_1)}{2} h(b_2) + \sqrt{2} \int_{b_1}^{b_2} h(s)\, ds \\ &\quad - \frac{3\sqrt{2}}{(d_2 - d_1)} \int_{b_1}^{b_2} \int_s^{b_2} h(u)\, du\, ds. \end{aligned} \quad (16)$$

3. H_∞ Control for Synchronization of Coronary Artery System

In this section, a novel synchronization criterion will be mentioned on chaotic coronary artery system, which can ensure that the error system asymptotically converges to the zero. In other words, the synchronization will be achieved between the normal and diseased blood vessels based on the following theorem.

Theorem 6. *Considering the states of error system (5) and Assumption 1, the error system (5) is asymptotical convergence to zero if there exist positive values r_m, r_M, r_d, κ_{12}, κ_{13}, κ_{14}, κ_{15}, positive symmetric matrices P, R_1, R_2, R_3, Q_1, Q_2, Q_3, Q_4, symmetric matrices M_1, M_3, and appropriate dimensions matric M_2, N_1, N_2, S_1, S_2, L, such that*

$$P = \begin{bmatrix} \overrightarrow{P}_{11} & \kappa_{12}\overrightarrow{P}_{11} & \kappa_{13}\overrightarrow{P}_{11} & \kappa_{14}\overrightarrow{P}_{11} & \kappa_{15}\overrightarrow{P}_{11} \\ * & \overrightarrow{P}_{22} & \overrightarrow{P}_{23} & \overrightarrow{P}_{24} & \overrightarrow{P}_{25} \\ * & * & \overrightarrow{P}_{33} & \overrightarrow{P}_{34} & \overrightarrow{P}_{35} \\ * & * & * & \overrightarrow{P}_{44} & \overrightarrow{P}_{45} \\ * & * & * & * & \overrightarrow{P}_{55} \end{bmatrix} \geq 0 \quad (P \in 5n * 5n), \tag{17}$$

$$\begin{bmatrix} \Psi & r_m^2\nu^T & r_{Mm}\nu^T & \frac{r_m^3}{2}\nu^T & \frac{r_{Mm}^3}{2}\nu^T & \overrightarrow{P}_{11} & \overrightarrow{P}_{11}L^T \\ * & -\overrightarrow{P}_{11}Q_1^{-1}\overrightarrow{P}_{11} & 0 & 0 & 0 & 0 & 0 \\ * & * & -\overrightarrow{P}_{11}Q_2^{-1}\overrightarrow{P}_{11} & 0 & 0 & 0 & 0 \\ * & * & * & -\overrightarrow{P}_{11}Q_3^{-1}\overrightarrow{P}_{11} & 0 & 0 & 0 \\ * & * & * & * & -\overrightarrow{P}_{11}Q_4^{-1}\overrightarrow{P}_{11} & 0 & 0 \\ * & * & * & * & * & -I & 0 \\ * & * & * & * & * & * & -I \end{bmatrix} < 0, \tag{18}$$

$$\begin{bmatrix} \widetilde{M}_1 & \widetilde{M}_2 & \widetilde{N}_1 \\ * & \widetilde{M}_3 & \widetilde{N}_2 \\ * & * & \widetilde{Q}_1 \end{bmatrix} \geq 0, \tag{19}$$

$$\begin{bmatrix} \widetilde{Q}_2 & \widetilde{S}_d \\ * & \widetilde{Q}_2 \end{bmatrix} \geq 0, \quad (d = 1, 2), \tag{20}$$

where

$$\Psi = \sum_{i=1}^{5}\left[\widetilde{\Upsilon}_i^T\widetilde{F}_i + \widetilde{F}_i^T\widetilde{\Upsilon}_i\right] + \widetilde{R} + \widetilde{H} + r_m^4\omega_1^T\left(M_1 + \frac{1}{3} \cdot M_3\right)\omega_1 + r_m^3\mathrm{sym}\left\{\omega_1^T N_1\omega_2 + \omega_1^T N_2\omega_3\right\} + \sum_{i=4}^{7}\omega_i^T\widetilde{Q}_2\omega_i - \omega_4^T\widetilde{S}_1\omega_6 - \omega_6^T\widetilde{S}_1^T\omega_4 - \omega_5^T\widetilde{S}_2\omega_7 - \omega_7^T\widetilde{S}_2^T\omega_5 - r_m^2\sum_{i=8}^{9}\omega_i^T\widetilde{Q}_3\omega_i - r_{Mm}^2\sum_{i=10}^{11}\omega_i^T\widetilde{Q}_4\omega_i,$$

$$\overrightarrow{P}_{11} = P_{11}^{-1},$$

$$\widetilde{\Upsilon}_1 = \nu = A\overrightarrow{P}_{11}n_1 + K\overrightarrow{P}_{11}n_3 + Cn_{11} + Dn_{12},$$

$$\widetilde{\Upsilon}_2 = n_1 - n_2,$$

$$\widetilde{\Upsilon}_3 = n_2 - n_4,$$

$$\widetilde{\Upsilon}_4 = r_m n_1 - n_5,$$

$$\widetilde{\Upsilon}_5 = r_{Mm}n_2 - n_6,$$

$$\widetilde{F}_1 = n_1 I + \kappa_{12}n_5 I + \kappa_{13}n_6 I + \kappa_{14}n_7 I + \kappa_{15}n_8 I,$$

$$\widetilde{F}_2 = \kappa_{12}\overrightarrow{P}_{11}n_1 + \overrightarrow{P}_{22}n_5 + \overrightarrow{P}_{23}n_6 + \overrightarrow{P}_{24}n_7 + \overrightarrow{P}_{25}n_8,$$

$$\widetilde{F}_3 = \kappa_{13}\overrightarrow{P}_{11}n_1 + \overrightarrow{P}_{23}^T n_5 + \overrightarrow{P}_{33}n_6 + \overrightarrow{P}_{34}n_7 + \overrightarrow{P}_{35}n_8,$$

$$\begin{aligned}
&\widetilde{F}_4 = \kappa_{14}\overrightarrow{P}_{11}n_1 + \overrightarrow{P}_{24}^T n_5 + \overrightarrow{P}_{34}^T n_6 + \overrightarrow{P}_{44}n_7 + \overrightarrow{P}_{45}n_8,\\
&\widetilde{F}_5 = \kappa_{15}\overrightarrow{P}_{11}n_1 + \overrightarrow{P}_{25}^T n_5 + \overrightarrow{P}_{35}^T n_6 + \overrightarrow{P}_{45}^T n_7 + \overrightarrow{P}_{55}n_8,\\
&\widetilde{R} = \operatorname{diag}\left\{\widetilde{R}_1 + \widetilde{R}_2 + \widetilde{R}_3, -\widetilde{R}_2, -\left(1 - r_d\right)\widetilde{R}_1,\right.\\
&\quad \left. -\widetilde{R}_3, 0, 0, 0, 0, 0, 0, 0, 0\right\},\\
&\widetilde{H} = H_1 + H_2 = \left\{I + L^T L, 0, 0, 0, 0, 0, 0, 0, 0, 0, -I,\right.\\
&\quad \left. -\beta^2 I\right\},\\
&\omega_1 = \left\{n_1, n_2, n_5\right\}^T,\\
&\omega_2 = n_1 - n_2,\\
&\omega_3 = 2n_5 - n_1 - n_2,\\
&\omega_4 = n_2 - n_3,\\
&\omega_5 = \sqrt{3}n_2 + \sqrt{3}n_3 - 2\sqrt{3}n_9,\\
&\omega_6 = n_3 - n_4,\\
&\omega_7 = \sqrt{3}n_3 + \sqrt{3}n_4 - 2\sqrt{3}n_{10},\\
&\omega_8 = r_m n_1 - n_5,\\
&\omega_9 = \frac{\sqrt{2}r_m}{2}n_1 + \sqrt{2}n_5 - \frac{3\sqrt{2}}{r_m}n_7,\\
&\omega_{10} = r_{Mm}n_2 - n_6,\\
&\omega_{11} = \frac{\sqrt{2}r_{Mm}}{2}n_2 + \sqrt{2}n_6 - \frac{3\sqrt{2}}{r_{Mm}}n_8,\\
&r_{Mm} = r_M - r_m,\\
&n_k\,(k = 1, \ldots, 12) \in R^{12n*n}\ \{e.g.\, n_2\\
&\quad = [0, 0, I, 0, 0, 0, 0, 0, 0, 0, 0, 0]\}.
\end{aligned} \tag{21}$$

Proof. LKF can be constructed as follows:

$$V(t) = \sum_{i=1}^{4} V_i(t), \tag{22}$$

where

$$V_1 = \varpi^T(t) P \varpi(t), \tag{23}$$

$$\begin{aligned}
V_2 &= \int_{t-r(t)}^{t} e^T(s) R_1 e(s)\, ds + \int_{t-r_m}^{t} e^T(s) R_2 e(s)\, ds\\
&\quad + \int_{t-r_M}^{t} e^T(s) R_3 e(s)\, ds,
\end{aligned} \tag{24}$$

$$\begin{aligned}
V_3 &= r_m^3 \int_{-r_m}^{0}\int_{t+s}^{t} \dot{e}^T(u) Q_1 \dot{e}(u)\, du\, ds\\
&\quad + r_{Mm}\int_{-r_M}^{-r_m}\int_{t+s}^{t} \dot{e}^T(u) Q_2 \dot{e}(u)\, du\, ds,
\end{aligned} \tag{25}$$

$$\begin{aligned}
V_4 &= \frac{r_m^4}{2}\int_{t-r_m}^{t}\int_{s}^{t}\int_{u}^{t} \dot{e}^T(v) Q_3 \dot{e}(v)\, dv\, du\, ds\\
&\quad + \frac{r_{Mm}^4}{2}\int_{t-r_M}^{t-r_m}\int_{s}^{t-r_m}\int_{u}^{t} \dot{e}^T(v) Q_4 \dot{e}(v)\, dv\, du\, ds,
\end{aligned} \tag{26}$$

$$\begin{aligned}
&\bar{\omega}^T(t) = \left[e(t), d_1(t), d_2(t), d_3(t), d_4(t)\right],\\
&d_1(t) = \int_{t-r_m}^{t} e^T(s)\, ds,\\
&d_2(t) = \int_{t-r_M}^{t-r_m} e^T(s)\, ds,\\
&d_3(t) = \int_{t-r_m}^{t}\int_{s}^{t} e^T(u)\, du\, ds,\\
&d_4(t) = \int_{t-r_M}^{t-r_m}\int_{s}^{t-r_m} e^T(u)\, du\, ds.
\end{aligned} \tag{27}$$

Based on the above condition, the derivative of $V(t)$ can be obtained:

$$\dot{V}(t) = \sum_{i=1}^{4} \dot{V}_i(t), \tag{28}$$

where

$$\begin{aligned}
\dot{V}_1(t) &= 2\dot{\bar{\omega}}^T(t) P \bar{\omega}(t) = 2\dot{e}^T(t)\left[P_{11}e(t) + \kappa_{12}P_{11}d_1\right.\\
&\quad \left. + \kappa_{13}P_{11}d_2 + \kappa_{14}P_{11}d_3 + \kappa_{14}P_{11}d_4\right] + 2\alpha_1^T(t)\\
&\quad \cdot \left[\kappa_{12}P_{11}^T e(t) + P_{22}d_1(t) + P_{23}d_2(t) + P_{24}d_3(t)\right.\\
&\quad \left. + P_{25}d_4(t)\right] + 2\alpha_2^T(t)\left[\kappa_{13}P_{11}^T e(t) + P_{23}^T d_1(t)\right.\\
&\quad \left. + P_{33}d_2(t) + P_{34}d_3(t) + P_{35}d_4(t)\right] + 2\alpha_3^T(t)\\
&\quad \cdot \left[\kappa_{14}P_{11}^T e(t) + P_{24}^T d_1(t) + P_{34}^T d_2(t) + P_{44}d_3(t)\right.\\
&\quad \left. + P_{45}d_4(t)\right] + 2\alpha_4^T(t)\left[\kappa_{15}P_{11}^T e(t) + P_{25}^T d_1(t)\right.\\
&\quad \left. + P_{35}^T d_2(t) + P_{45}^T d_3(t) + P_{55}d_4(t)\right] = \eta^T(t)\\
&\quad \cdot \sum_{i=1}^{5} \operatorname{sym}\left\{\Upsilon_i^T F_i\right\}\eta(t),
\end{aligned} \tag{29}$$

$$\dot{V}_2(t) = \sum_{i=1}^{3} e^T(t) R_i e(t) - (1-\dot{r}(t)) e^T(t-r(t)) \cdot R_1 e(t-r(t)) - e^T(t-r_m) R_2 e(t-r_m) - e^T(t-r_M) R_3 e(t-r_M) \le \eta^T(t) R \eta(t), \tag{30}$$

$$\dot{V}_3(t) = \dot{e}^T(t) \left[r_m^4 Q_1 + r_{Mm}^2 Q_2\right] \dot{e}(t) + \sum_{i=1}^{3} \xi_i = \eta^T(t) \cdot \nu^T W_1 \nu \eta(t) + \sum_{i=1}^{3} \xi_i, \tag{31}$$

$$\dot{V}_4(t) = \frac{r_m^4}{2} \int_{t-r_m}^{t} \int_{s}^{t} \left[\dot{e}^T(t) Q_3 \dot{e}(t) - \dot{e}^T(u) Q_3 \dot{e}(u)\right] du\, ds + \frac{r_{Mm}^4}{2} \cdot \int_{t-r_M}^{t-r_m} \int_{s}^{t-r_m} \left[\dot{e}^T(t) Q_4 \dot{e}(t) - \dot{e}^T(u) Q_4 \dot{e}(u)\right] du\, ds = \eta^T(t) \cdot \nu^T W_2 \nu \eta(t) + \sum_{i=4}^{5} \xi_i, \tag{32}$$

with

$$\eta^T(t) = \left\{e^T(t), e^T(t-r_m), e^T(t-r(t)), e^T(t-r_M), d_1(t), d_2(t), d_3(t), d_4(t), d_5(t), d_6(t), f^T(t), \varrho^T(t)\right\},$$

$$\alpha_1 = e(t) - e(t-r_m),$$

$$\alpha_2 = e(t-r_m) - e(t-r_M),$$

$$\alpha_3 = r_m e(t) - d_1(t),$$

$$\alpha_4 = r_{Mm} e(t-r_m) - d_2(t),$$

$$\Upsilon_1 = A n_1 + A_1 n_3 + C n_{11} + D n_{12},$$

$$\Upsilon_2 = n_1 - n_2,$$

$$\Upsilon_3 = n_2 - n_4,$$

$$\Upsilon_4 = r_m n_1 - n_5,$$

$$\Upsilon_5 = r_{Mm} n_2 - n_6,$$

$$F_1 = P_{11} n_1 + \kappa_{12} P_{11} n_5 + \kappa_{13} P_{11} n_6 + \kappa_{14} P_{11} n_7 + \kappa_{15} P_{11} n_8,$$

$$F_2 = \kappa_{12} P_{11}^T n_1 + P_{22} n_5 + P_{23} n_6 + P_{24} n_7 + P_{25} n_8,$$

$$F_3 = \kappa_{13} P_{11}^T n_1 + P_{23}^T n_5 + P_{33} n_6 + P_{34} n_7 + P_{35} n_8,$$

$$F_4 = \kappa_{14} P_{11}^T n_1 + P_{24}^T n_5 + P_{34}^T n_6 + P_{44} n_7 + P_{45} n_8,$$

$$F_5 = \kappa_{15} P_{11}^T n_1 + P_{25}^T n_5 + P_{35}^T n_6 + P_{45}^T n_7 + P_{55} n_8,$$

$$R = \operatorname{diag}\{R_1 + R_2 + R_3, -R_2, -(1-r_d) R_1, -R_3, 0, 0, 0, 0, 0, 0, 0, 0\},$$

$$W_1 = r_m^4 Q_1 + r_{Mm}^2 Q_2,$$

$$W_2 = \frac{r_m^6}{4} Q_3 + \frac{r_{Mm}^6}{4} Q_4,$$

$$\nu = A n_1 + K n_3 + C n_{11} + D n_{12},$$

$$\xi_1 = -r_m^3 \int_{t-r_m}^{t} \dot{e}^T(s) Q_1 \dot{e}(s)\, ds,$$

$$\xi_2 = -r_{Mm} \int_{t-r(t)}^{t-r_m} \dot{e}^T(s) Q_2 \dot{e}(s)\, ds,$$

$$\xi_3 = -r_{Mm} \int_{t-r_M}^{t-r(t)} \dot{e}^T(s) Q_2 \dot{e}(s)\, ds,$$

$$\xi_4 = -\frac{r_m^4}{2} \int_{t-r_m}^{t} \int_{s}^{t} \dot{e}^T(u) Q_3 \dot{e}(u)\, du\, ds,$$

$$\xi_5 = -\frac{r_{Mm}^4}{2} \int_{t-r_M}^{t-r_m} \int_{s}^{t-r_m} \dot{e}^T(u) Q_4 \dot{e}(u)\, du\, ds,$$

$$d_5(t) = \frac{1}{r(t) - r_m} \int_{t-r(t)}^{t-r_m} e^T(s)\, ds,$$

$$d_6(t) = \frac{1}{r_M - r(t)} \int_{t-r(M)}^{t-r(t)} e^T(s)\, ds. \tag{33}$$

According to Lemmas 2 and 3, we can get

$$\begin{bmatrix} M_1 & M_2 & N_1 \\ * & M_3 & N_2 \\ * & * & Q_1 \end{bmatrix} \ge 0, \tag{34}$$

$$\xi_1(t) \le r_m^4 \upsilon_1^T(t-r_m, t) \left[M_1 + \frac{1}{3} M_3\right] \upsilon_1(t, t-r_m) + r_m^3 \operatorname{sym}\left\{\upsilon_1^T(t-r_m, t) N_1 \upsilon_2(t-r_m, t) + \upsilon_1^T(t-r_m, t) N_2 \upsilon_3(t-r_m, t)\right\}, \tag{35}$$

$$\xi_2(t) \le -\frac{1}{\theta_1} \left[\upsilon_4^T(t) Q_2 \upsilon_4(t) + \upsilon_5^T(t) Q_2 \upsilon_5(t)\right], \tag{36}$$

$$\xi_3(t) \le -\frac{1}{\theta_2} \left[\upsilon_6^T(t) Q_2 \upsilon_6(t) + \upsilon_7^T(t) Q_2 \upsilon_7(t)\right], \tag{37}$$

where

$$\theta_1 = \frac{r(t) - r_m}{r_{Mm}},$$

$$\theta_2 = \frac{r_M - r(t)}{r_{Mm}},$$

$$\upsilon_1 = \left[e^T(t), e^T(t-r_m), \frac{1}{r_m} \int_{t-r_m}^{t} e^T(s)\, ds\right],$$

$$
\begin{aligned}
v_2 &= e^T(t) - e^T(t - r_m),\\
v_3 &= \frac{2}{r_m}\int_{t-r_m}^{t} e^T(s)\,ds - e^T(t) - e^T(t - r_m),\\
v_4 &= e(t - r_m) - e(t - r(t)),\\
v_5 &= \sqrt{3}e(t - r_m) + \sqrt{3}e(t - r(t)) - 2\sqrt{3}d_5(t),\\
v_6 &= e(t - r(t)) - e(t - r_M),\\
v_7 &= \sqrt{3}e(t - r(t)) + \sqrt{3}e(t - r_M) - 2\sqrt{3}d_6(t).
\end{aligned}
\tag{38}
$$

From inequality (35), we have

$$
\begin{aligned}
\xi_1(t) \le \eta^T(t) r_m^3 \Big\{ & r_m \omega_1^T \left[M_1 + \frac{1}{3}M_3\right]\omega_1\\
& + \operatorname{sym}\left[\omega_1^T N_1 \omega_2 + \omega_1^T N_2 \omega_3\right]\Big\}\eta(t).
\end{aligned}
\tag{39}
$$

The real numbers θ_1, θ_2 satisfy $\theta_1 > 0, \theta_2 > 0$, and $\theta_1 + \theta_2 = 1$. Then appropriate dimensions matrices S_1, S_2 are introduced, such that

$$
\begin{bmatrix} Q_2 & S_1 \\ * & Q_2 \end{bmatrix} \ge 0,
\qquad
\begin{bmatrix} Q_2 & S_2 \\ * & Q_2 \end{bmatrix} \ge 0.
\tag{40}
$$

Applying Lemma 4 to inequalities (36) (37), we have

$$
\begin{aligned}
\xi_2(t) + \xi_3(t) \le & -\left(\frac{1}{\theta_1} v_4^T(t) Q_2 v_4(t) + \frac{1}{\theta_2} v_6^T(t) Q_2 v_6(t)\right) - \left(\frac{1}{\theta_1} v_5^T(t) Q_2 v_5(t) + \frac{1}{\theta_2} v_7^T(t) Q_2 v_7(t)\right)\\
\le & -\begin{bmatrix} v_4(t) \\ v_6(t) \end{bmatrix}^T \cdot \begin{bmatrix} Q_2 & S_1 \\ * & Q_2 \end{bmatrix}\begin{bmatrix} v_4(t) \\ v_6(t) \end{bmatrix} - \begin{bmatrix} v_5(t) \\ v_7(t) \end{bmatrix}^T \cdot \begin{bmatrix} Q_2 & S_2 \\ * & Q_2 \end{bmatrix}\begin{bmatrix} v_5(t) \\ v_7(t) \end{bmatrix}\\
= & -\eta^T(t)\left[\sum_{i=4}^{7}\omega_i^T Q_2 \omega_i + \omega_4^T S_1 \omega_6 + \omega_6^T S_1^T \omega_4 + \omega_5^T S_2 \omega_7 + \omega_7^T S_2^T \omega_5\right]\eta(t).
\end{aligned}
\tag{41}
$$

Using Lemma 5, $\xi_4(t)$, $\xi_5(t)$ can be transformed as follows:

$$
\begin{aligned}
\xi_4(t) &\le -r_m^2 \begin{bmatrix} \tau_1(t) \\ \tau_2(t) \end{bmatrix}^T \begin{bmatrix} Q_3 & 0 \\ * & Q_3 \end{bmatrix}\begin{bmatrix} \tau_1(t) \\ \tau_2(t) \end{bmatrix}\\
&= -\eta^T(t) r_m^2 \sum_{i=8}^{9} \omega_i^T Q_3 \omega_i \eta(t),\\
\xi_5(t) &\le -r_{Mm}^2 \begin{bmatrix} \tau_3(t) \\ \tau_4(t) \end{bmatrix}^T \begin{bmatrix} Q_4 & 0 \\ * & Q_4 \end{bmatrix}\begin{bmatrix} \tau_3(t) \\ \tau_4(t) \end{bmatrix}\\
&= -\eta^T(t) r_{Mm}^2 \sum_{i=10}^{11} \omega_i^T Q_4 \omega_i \eta(t),
\end{aligned}
\tag{42}
$$

where

$$
\begin{aligned}
\tau_1(t) &= r_m e(t) - d_1(t),\\
\tau_2(t) &= \frac{\sqrt{2} r_m}{2} 2(t) + \sqrt{2} d_1(t) - \frac{3\sqrt{2}}{r_m} d_3(t),\\
\tau_3(t) &= r_{Mm} e(t - r_m) - d_2(t),\\
\tau_4(t) &= \frac{\sqrt{2} r - Mm}{2} e(t - r_m) + \sqrt{2} d_2(t) - \frac{3\sqrt{2}}{r_{Mm}} d_4(t),
\end{aligned}
\tag{43}
$$

Next, we define a performance index $J(e(t), \varrho(t))$ to study H_∞ performance:

$$
J(e(t), \varrho(t)) = \int_0^\infty \left[e^T(u) e(u) - \beta^2 \varrho^T(u) \varrho(u)\right] du.
\tag{44}
$$

Under the zero initial conditions, we can obtain

$$
\begin{aligned}
J(e(t), \varrho(t)) &= \int_0^\infty \left[e^T(t) e(t) - \beta^2 \varrho^T(t) \varrho(t) + \dot{V}(t)\right] dt\\
&\quad - V(t)\Big|_{t\to\infty} \le \int_0^\infty \left[e^T(t) e(t) - \beta^2 \varrho^T(t) \varrho(t) + \dot{V}(t)\right] dt = \int_0^\infty \eta^T(t)\left\{\Delta + \nu^T\left(W_1 + W_2\right)\nu\right\}\\
&\quad \cdot \eta(t)\, dt,
\end{aligned}
\tag{45}
$$

where

$$
\Delta = \sum_{i=1}^{5}\left[\Upsilon_i^T F_i + F_i^T \Upsilon_i\right] + R + H_1 + H_2 + r_m^4 \omega_1^T \left(M_1 + \frac{1}{3}M_3\right)\omega_1
$$

$$
\begin{aligned}
&+ r_m^3 \operatorname{sym}\left\{\omega_1^T N_1 \omega_2 + \omega_1^T N_2 \omega_3\right\} \\
&+ \sum_{i=4}^{7} \omega_i^T \widetilde{Q}_2 \omega_i - \omega_4^T S_1 \omega_6 - \omega_6^T S_1^T \omega_4 - \omega_5^T S_2 \omega_7 \\
&- \omega_7^T S_2^T \omega_5 - r_m^2 \sum_{i=8}^{9} \omega_i^T Q_3 \omega_i \\
&- r_{Mm}^2 \sum_{i=10}^{11} \omega_i^T Q_4 \omega_i, \\
H_1 &= \operatorname{diag}\left\{L^T L, 0, 0, 0, 0, 0, 0, 0, 0, 0, 0, -I, 0\right\}, \\
H_2 &= \operatorname{diag}\left\{I, 0, 0, 0, 0, 0, 0, 0, 0, 0, 0, -\beta^2 I\right\}.
\end{aligned} \tag{46}
$$

Ordering disturbance attenuation parameter $\beta > 0$ and matric $\Psi = \Delta + \nu^T(W_1 + W_2)\nu$, we can get

$$
J\left(e(t), \varrho(t)\right) \le \eta^T(t)\,\Psi\eta(t). \tag{47}
$$

To apply congruence transform, multiplying both sides of Ψ with $\operatorname{diag}(\underbrace{P_{11}^{-1}, \ldots, P_{11}^{-1}}_{10}, I, I)$ and employing Schur complements, inequality (18) can be induced. Similarly, multiplying both sides of matric (34) with $\operatorname{diag}(\underbrace{P_{11}^{-1}, \ldots, P_{11}^{-1}}_{7})$ and matric (40) with $\operatorname{diag}(P_{11}^{-1}, P_{11}^{-1})$, we can get inequality (19) (20), where

$$
\begin{aligned}
\widetilde{Q}_x &= \overrightarrow{P}_{11}\widetilde{Q}_x\overrightarrow{P}_{11}, \quad (x = 1,2,3,4), \\
\widetilde{R}_y &= \overrightarrow{P}_{11}\widetilde{R}_y\overrightarrow{P}_{11}, \\
\widetilde{M}_y &= \overrightarrow{P}_{11}\widetilde{M}_y\overrightarrow{P}_{11}, \quad (y = 1,2,3), \\
\widetilde{N}_d &= \overrightarrow{P}_{11}\widetilde{N}_d\overrightarrow{P}_{11}, \\
\widetilde{S}_d &= \overrightarrow{P}_{11}\widetilde{S}_d\overrightarrow{P}_{11}, \\
\widetilde{H}_d &= \overrightarrow{P}_{11}\widetilde{H}_d\overrightarrow{P}_{11}, \quad (d = 1,2), \\
\overrightarrow{P}_{ij} &= \overrightarrow{P}_{11}P_{ij}\overrightarrow{P}_{11} \quad (i,j = 1,2,3,4,5), \\
F &= K\overrightarrow{P}_{11}.
\end{aligned} \tag{48}
$$

This completes the proof. □

Due to presence of nonlinear terms in the form of $\overrightarrow{P}_{11}Q_x\overrightarrow{P}_{11}$ $(x = 1,2,3,4)$, we cannot obtain a feasible solution by LMI tool box. To solve this problem, the cone complementary linearization algorithm (CCLA) is proposed [23]. Define new variable T_x $(x = 1,2,3,4)$ satisfying

$$
\overrightarrow{P}_{11}\widetilde{Q}_x\overrightarrow{P}_{11} \ge T_x \quad (x = 1,2,3,4). \tag{49}
$$

Applying Schur complements, expression (49) can be induced as follows:

$$
\begin{bmatrix} -\widetilde{Q}_x^{-1} & \overrightarrow{P}_{11}^{-1} \\ * & -T_x^{-1} \end{bmatrix} \le 0, \quad (x = 1,2,3,4). \tag{50}
$$

Set $Y_x = \widetilde{Q}_x^{-1}$, $P_n = \overrightarrow{P}_{11}^{-1}$, $U_x = T_x^{-1}$. From (50), we have

$$
\begin{bmatrix} -Y_x & P_n \\ * & -U_x \end{bmatrix} \le 0, \quad (x = 1,2,3,4). \tag{51}
$$

Then, the nonlinear optimization problem can be represented:

$$
\min \operatorname{tr}\left(\overrightarrow{P}_{11}P_n + \sum_{x=1}^{4}\left(Y_xQ_x + U_xT_x\right)\right), \tag{52}
$$

subject to formulas (18)–(20) and (51):

$$
\begin{bmatrix}
\Psi & r_m^2\nu^T & r_{Mm}\nu^T & \frac{r_m^3}{2}\nu^T & \frac{r_{Mm}^3}{2}\nu^T & \overrightarrow{P}_{11} & \overrightarrow{P}_{11}L^T \\
* & -G_1 & 0 & 0 & 0 & 0 & 0 \\
* & * & -G_2 & 0 & 0 & 0 & 0 \\
* & * & * & -G_3 & 0 & 0 & 0 \\
* & * & * & * & -G_4 & 0 & 0 \\
* & * & * & * & * & -I & 0 \\
* & * & * & * & * & * & -I
\end{bmatrix}, \tag{53}
$$

$$
\begin{aligned}
&\begin{bmatrix} \overrightarrow{P}_{11} & I \\ * & P_n \end{bmatrix} \ge 0, \\
&\begin{bmatrix} Y_x & I \\ * & \widetilde{Q}_x \end{bmatrix} \ge 0, \\
&\begin{bmatrix} U_x & I \\ * & T_x \end{bmatrix} \ge 0, \\
&\qquad (x = 1,2,3,4).
\end{aligned} \tag{54}
$$

Thus, the minimization problem (53) (54) can be solved by the following iterative algorithm.

Algorithm 7. (i) For given scalars $r_m, r_M, r_d, \kappa_{1j}$ $(j = 2,3,4,5)$, find a feasible set $(\overrightarrow{P}_{11}^0, P_n^0, Y_x, \widetilde{Q}_x^0, U_x^0, T_x^0, F^0)$ of LMI in (54). If there is none, exit. Set $b = 0$. (ii) Solve minimization problem with a feasible set:

$$
\left(\overrightarrow{P}_{11}^0, P_n^0, Y_x, \widetilde{Q}_x^0, U_x^0, T_x^0, F^0\right). \tag{55}
$$

Minimize

$$
\begin{aligned}
&\operatorname{tr}\Bigg(\overrightarrow{P}_{11}^b P_n + P_n^b\overrightarrow{P}_{11} \\
&\quad + \sum_{x=1}^{4}\left(Y_x^b\widetilde{Q}_x + \widetilde{Q}_x^bY_x + U_x^bT_x + T_x^bU_x\right)\Bigg)
\end{aligned} \tag{56}
$$

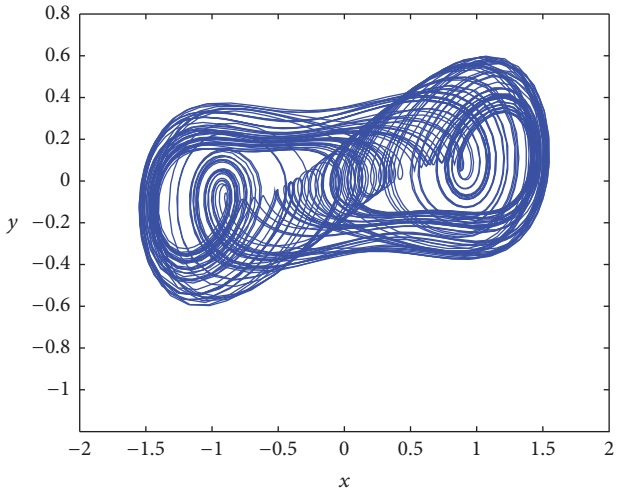

Figure 1: The trajectory of chaotic coronary artery system without disturbance and controller.

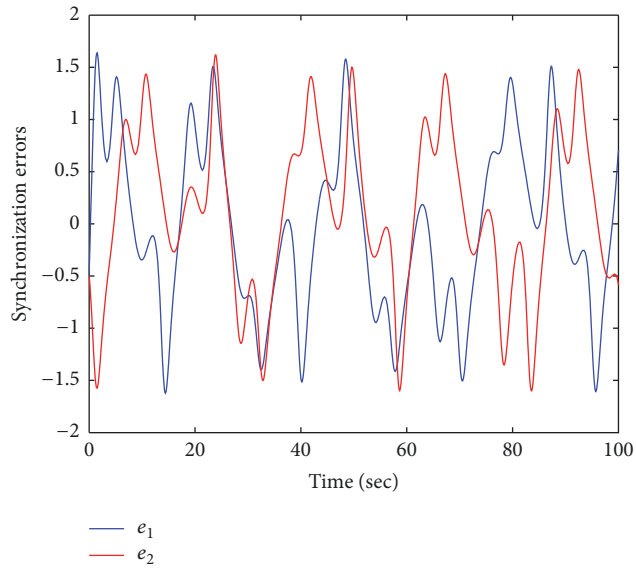

Figure 2: State responses of error system (5) without controller.

subject to LMI (54). Set $\overrightarrow{P}_{11}^{b+1} = \overrightarrow{P}_{11}$, $P_n^{b+1} = P_n$, $Y_x^{b+1} = Y_x$, $\widetilde{Q}_x^{b+1} = \widetilde{Q}_x$, $U_x^{b+1} = U_x$, $T_x^{b+1} = T_x$, $F^{b+1} = F$. (iii) If linear matrix inequalities (18)–(20) are feasible for $K = F\overrightarrow{P}_{11}^{-1}$, then drop out. Otherwise, set $b = b + 1$ and go to item (ii).

4. Simulation

The simulation will be exploited to express the effectiveness of the above theoretical results. To simulate normal states of blood vessel, give the parameters $c = 0.15$, $d = -1.7$, $E = 0.3$, $\omega = 1$ [12]. The chaotic response can be diversiform with the change of τ. It means that the changes of pathological blood vessels may be induced by different parameter τ. As $\tau = -0.5$, coronary artery system (1) will show the very complex dynamic behavior. The bifurcation diagram of system (1) is shown in Figure 1 without external disturbance and controller. The single and double nitrate isosorbide nitrate (controller u) is quickly absorbed by patients; blood vessels will dilate and increase blood supply to the heart muscle, which effectively relieves angina symptoms. To demonstrate the fact, order initial matrices A, C, D, L and the initial state vectors $x_m(0)$, $x_s(0)$ as follows:

$$A = \begin{bmatrix} -0.15 & 1.7 \\ 0.575 & -0.35 \end{bmatrix},$$

$$C = \begin{bmatrix} 5 & 0 \\ 0 & 5 \end{bmatrix},$$

$$D = \begin{bmatrix} 1 & 0 \\ 0 & 1 \end{bmatrix},$$

$$L = \begin{bmatrix} 0 & 0 \\ 0 & 0.36 \end{bmatrix},$$

$$x_m(0) = [0.5, 0],$$
$$x_s(0) = [-1, 1.5]. \tag{57}$$

Then, to solute chaotic behavior and investigate external disturbance on the system performance, the control signal $u(t)$ and the external disturbance signal $\varrho(t)$ are imposed on system (3), where $\varrho(t) = [\sin(40t), \sin(30t)]$. For simplicity of calculation, order $\kappa_{12}, \kappa_{13}, \kappa_{14}, \kappa_{15} = 0$. Based on the above condition, Figure 2 shows the trajectories and error states of error system without controller $u(t)$, which illustrates synchronization error is not asymptotical to approach zero, where $e_i(t) = x_{si} - x_{mi}$ $(i = 1, 2)$ represent the inner radius deviation and the pressure changes between healthy and pathological system; thus the states of abnormal system are not gradually tracking the normal states without controller $u(t)$. In order to synchronize the above systems, we formulate H_∞ control strategy with the conditions of $r_m = 0.05$, $r_M = 0.25$, $r_d = 0.2$ and obtain the three situations of controller gain matrices. (i) When input time-delay $r(t) = 0.02 + 0.1s\sin(t)$ and disturbance attenuation parameter $\beta = 0.38$ applying Theorem 6, we can get

$$K_1 = \begin{bmatrix} 0.6959 & 0.1733 \\ 0.1715 & 0.6175 \end{bmatrix}. \tag{58}$$

The response of system (5) with $u(t)$ is revealed in Figure 3. (ii) When input time-delay $r(t) = 0.095 + 0.09\sin(t)$ and disturbance attenuation parameter $\beta = 0.39$ applying Theorem 6, we can get

$$K_2 = \begin{bmatrix} 0.7510 & 0.2096 \\ 0.2075 & 0.6550 \end{bmatrix}. \tag{59}$$

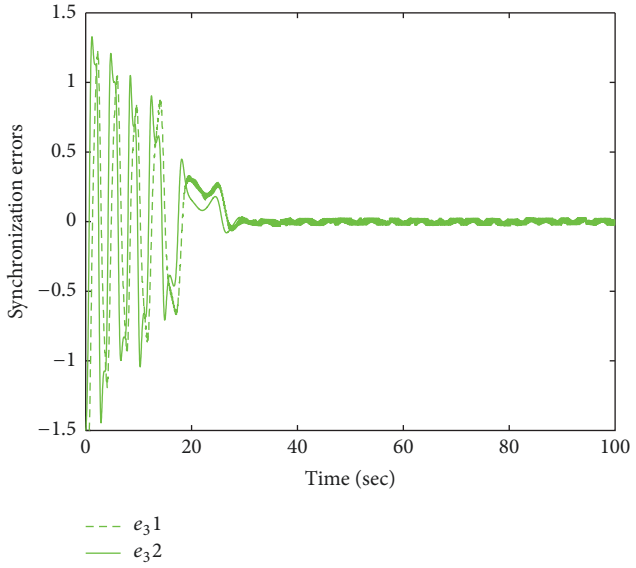

Figure 3: State responses of error system (5) with controller gain matrix K_1.

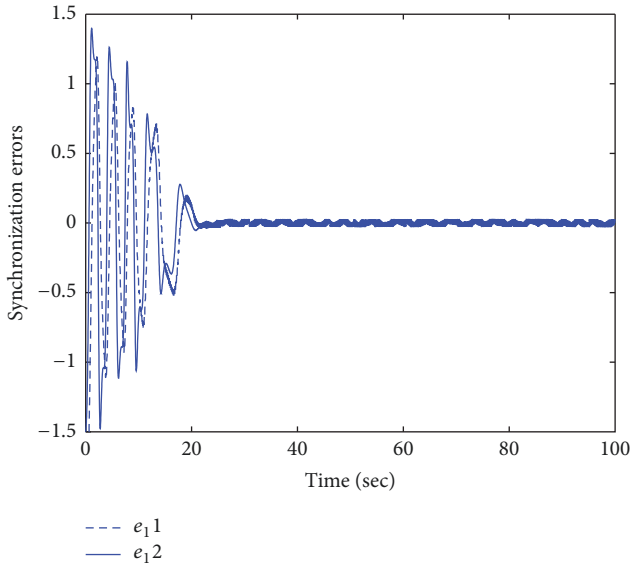

Figure 4: State responses of error system (5) with controller gain matrix K_2.

The response of system (5) with $u(t)$ is revealed in Figure 4. (iii) When input time-delay $r(t) = 0.1 + 0.1\sin(t)$ and disturbance attenuation parameter $\beta = 0.40$ applying Theorem 6, we can get

$$K_3 = \begin{bmatrix} 0.7563 & 0.2038 \\ 0.2017 & 0.6620 \end{bmatrix} \tag{60}$$

The response of system (5) with $u(t)$ is revealed in Figure 5. Under the effect of the aforementioned controller, we can see that the error system asymptotically converges to the zero

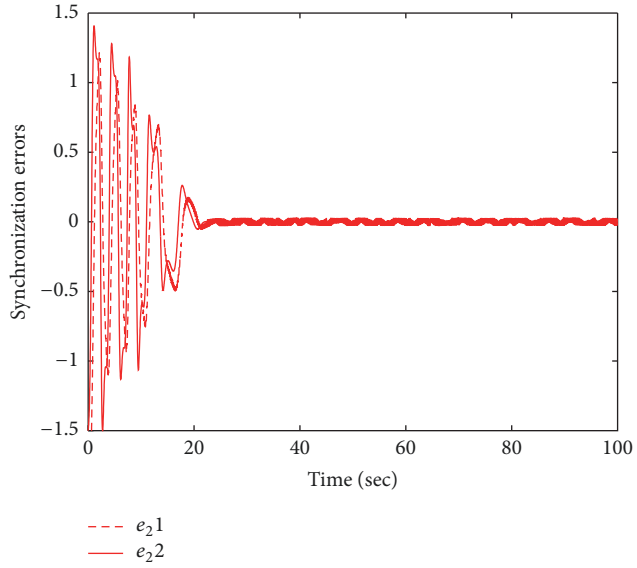

Figure 5: State responses of error system (5) with controller gain matrix K_3.

in Figures 3–5, which shows that the states of pathological system are gradually tracking the healthy states. As we can see from Figure 5, H_∞ control can reduce the effect of the disturbance signal $\varrho(t)$ and drive unhealthy vessel into the normal orbit in the shortest time, when given input time-delay $r(t) = 0.1 + 0.1\sin(t)$ and disturbance attenuation parameter $\beta = 0.40$. It is seen that the strategy of H_∞ control is efficient for the synchronization of coronary artery input time-delay system with external disturbance. Hence, the method has some theory and practice value for the treatment of angina symptoms. In addition, our approaches are advantageous in many input time-delay circumstances and it is worthless to elaborate in all aspects for brevity.

5. Conclusions

This paper has studied the problem of H_∞ control for synchronization of the coronary artery input time-delay system with disturbance. Based on triple integral form of Lyapunov-Krasovskii functionals, a sufficient condition has been established to ensure asymptotical convergence to zero for the error system under a given H_∞ performance level. Moreover, the free-matrix-based integral inequality, Wirtinger-based integral inequality, and reciprocal convex combination approach are used to obtain less conservatism. Furthermore, a novel H_∞ controller guaranteeing synchronization for master-slave system is designed under the above proposed conditions, which means the states of pathological vessel are gradually tracking the healthy states. Finally, simulation result demonstrates the effectiveness and feasibility of the presented strategies. Meanwhile, the research is especially significant to cure angina symptoms. In the future, we hope those methods can be further utilized for other time-delay systems.

Conflicts of Interest

The authors declare that there are no conflicts of interest regarding the publication of this paper.

Acknowledgments

This work was supported by National Natural Science Foundation of China (Grants nos. 61503280, 61403278, and 61402329) and Technology Commission of Tianjin Municipality (Grant no. 15JCYBJC16100).

References

[1] B. Chen, Y. Niu, and Y. Zou, "Adaptive sliding mode control for stochastic Markovian jumping systems with actuator degradation," *Automatica*, vol. 49, no. 6, pp. 1748–1754, 2013.

[2] Y. Li, S. Tong, L. Liu, and G. Feng, "Adaptive output-feedback control design with prescribed performance for switched nonlinear systems," *Automatica*, vol. 80, pp. 225–231, 2017.

[3] H. Wang and Q. Zhu, "Finite-time stabilization of high-order stochastic nonlinear systems in strict-feedback form," *Automatica*, vol. 54, pp. 284–291, 2015.

[4] H. Li, J. Wang, L. Wu, H. K. Lam, and Y. Gao, "Optimal guaranteed cost sliding mode control of interval type-2 fuzzy time-delay systems," *IEEE Transactions on Fuzzy Systems*, 2017.

[5] V. K. Yadav, S. Das, B. S. Bhadauria, A. K. Singh, and M. Srivastava, "Stability analysis, chaos control of a fractional order chaotic chemical reactor system and its function projective synchronization with parametric uncertainties," *Chinese Journal of Physics*, vol. 55, no. 3, pp. 594–605, 2017.

[6] F. Zouari, A. Boulkroune, and A. Ibeas, "Neural adaptive quantized output-feedback control-based synchronization of uncertain time-delay incommensurate fractional-order chaotic systems with input nonlinearities," *Neurocomputing*, vol. 237, pp. 200–225, 2017.

[7] W. Wei, M. Wang, D. Li, M. Zuo, and X. Wang, "Disturbance observer based active and adaptive synchronization of energy resource chaotic system," *ISA Transactions®*, vol. 65, pp. 164–173, 2016.

[8] K. Shi, X. Liu, H. Zhu, S. Zhong, Y. Zeng, and C. Yin, "Novel delay-dependent master-slave synchronization criteria of chaotic Lur'e systems with time-varying-delay feedback control," *Applied Mathematics and Computation*, vol. 282, pp. 137–154, 2016.

[9] H. Y. Li, Y. K. Wong, W. L. Chan, and K. M. Tsang, "Synchronization of Ghostburster neurons under external electrical stimulation via adaptive neural network H control," *Neurocomputing*, vol. 74, no. 1-3, pp. 230–238, 2010.

[10] H. Li, J. Wang, H. Du, and H. R. Karimi, "Adaptive sliding mode control for Takagi-Sugeno fuzzy systems and its applications," *IEEE Transactions on Fuzzy Systems*, 2017.

[11] L. Wang, H. Li, Q. Zhou, and R. Lu, "Adaptive fuzzy control for nonstrict feedback systems with unmodeled dynamics and fuzzy dead zone via output feedback," *IEEE Transactions on Cybernetics*, vol. 47, no. 9, pp. 2400–2412, 2017.

[12] C.-J. Lin, S.-K. Yang, and H.-T. Yau, "Chaos suppression control of a coronary artery system with uncertainties by using variable structure control," *Computers & Mathematics with Applications*, vol. 64, no. 5, pp. 988–995, 2012.

[13] Z. Zhao, X. Li, J. Zhang, and Y. Pei, "Terminal sliding mode control with self-tuning for coronary artery system synchronization," *International Journal of Biomathematics*, vol. 10, no. 3, Article ID 1750041, 2017.

[14] H. Li, L. Bai, Q. Zhou, R. Lu, and L. Wang, "Adaptive fuzzy control of stochastic nonstrict-feedback nonlinear systems with input saturation," *IEEE Transactions on Systems, Man, and Cybernetics: Systems*, vol. 47, no. 8, pp. 2185–2197, 2017.

[15] D. Zeng, R. Zhang, Y. Liu, and S. Zhong, "Sampled-data synchronization of chaotic Lur'e systems via input-delay-dependent-free-matrix zero equality approach," *Applied Mathematics and Computation*, vol. 315, pp. 34–46, 2017.

[16] M. Zhao and J. Wang, "H∞ control of a chaotic finance system in the presence of external disturbance and input time-delay," *Applied Mathematics and Computation*, vol. 233, pp. 320–327, 2014.

[17] S.-J. Fan, "Jensen's inequality for filtration consistent nonlinear expectation without domination condition," *Journal of Mathematical Analysis and Applications*, vol. 345, no. 2, pp. 678–688, 2008.

[18] É. Gyurkovics, "A note on Wirtinger-type integral inequalities for time-delay systems," *Automatica*, vol. 61, pp. 44–46, 2015.

[19] W.-J. Lin, Y. He, C.-K. Zhang, M. Wu, and M.-D. Ji, "Stability analysis of recurrent neural networks with interval time-varying delay via free-matrix-based integral inequality," *Neurocomputing*, vol. 205, pp. 490–497, 2016.

[20] K. Liu, E. Fridman, K. H. Johansson, and Y. Xia, "Generalized Jensen inequalities with application to stability analysis of systems with distributed delays over infinite time-horizons," *Automatica*, vol. 69, pp. 222–231, 2016.

[21] J.-H. Kim, "Further improvement of Jensen inequality and application to stability of time-delayed systems," *Automatica*, vol. 64, pp. 121–125, 2016.

[22] M. Park, O. Kwon, J. H. Park, S. Lee, and E. Cha, "Stability of time-delay systems via Wirtinger-based double integral inequality," *Automatica*, vol. 55, pp. 204–208, 2015.

[23] Y. Liu and M. Li, "Improved robust stabilization method for linear systems with interval time-varying input delays by using Wirtinger inequality," *ISA Transactions*, vol. 56, pp. 111–122, 2015.

[24] H.-B. Zeng, Y. He, M. Wu, and J. She, "Free-matrix-based integral inequality for stability analysis of systems with time-varying delay," *Institute of Electrical and Electronics Engineers Transactions on Automatic Control*, vol. 60, no. 10, pp. 2768–2772, 2015.

[25] P. Park, J. W. Ko, and C. Jeong, "Reciprocally convex approach to stability of systems with time-varying delays," *Automatica*, vol. 47, no. 1, pp. 235–238, 2011.

[26] T. M. Griffith and D. H. Edwards, "Fractal analysis of role of smooth muscle Ca2+ fluxes in genesis of chaotic arterial pressure oscillations," *American Journal of Physiology-Heart and Circulatory Physiology*, vol. 266, no. 5, pp. H1801–H1811, 1994.

[27] P. Roy, S. Ray, and S. Bhattacharya, "Synchronization of two chaotic coronary artery systems using modified feedback method," in *Proceedings of the 2nd International Conference on Control, Instrumentation, Energy and Communication, CIEC 2016*, pp. 145–148, India, January 2016.

[28] C.-C. Wang and H.-T. Yau, "Chaos analysis and synchronization control of coronary artery systems," *Abstract and Applied Analysis*, vol. 2013, Article ID 209718, 2013.

[29] Y. Shi, "Chaos and control in coronary artery system," *Discrete Dynamics in Nature and Society*, vol. 2012, Article ID 631476, 2012.

[30] A. Seuret and F. Gouaisbaut, "Wirtinger-based integral inequality: Application to time-delay systems," *Automatica*, vol. 49, no. 9, pp. 2860–2866, 2013.